JOURNAL OF SOLID STATE CHEMISTRY 63, 62–69 (1986)

Crystal Structure and Physical Properties of $EuMo_6S_8$ Single Crystals at Ambient Pressure

O. PEÑA,[1] R. HORYN,[2] C. GEANTET, P. GOUGEON, J. PADIOU, AND M. SERGENT

Laboratoire de Chimie Minérale B, Unité Associée au CNRS No. 254
Université de Rennes I, 35042 Rennes Cédex, France

Received July 23, 1985; in revised form October 9, 1985

X-Ray analyses were performed at room temperature on single crystals of $Eu_xMo_6S_8$. Refinement of its crystal structure shows an upper stoichiometry of $x = 1.0$. Atomic positions and crystallographic data are given in full. Crystals were also characterized through their susceptibility and transport properties. All europium atoms are divalent as confirmed by the magnetization at low temperatures. A well-defined anomaly on the electrical resistivity at $T_s = 107$ K separates the metallic high-temperature rhombohedral phase from the low-temperature nonmetallic (triclinic) phase. Very large residual resistivity ratios obtained for stoichiometric crystals favor our interpretation that the $Eu_{1.0}Mo_6S_8$ low-temperature phase must be essentially semiconducting. © 1986 Academic Press, Inc.

Introduction

The ternary metal molybdenum chalcogenides (Me–Mo–X) known as Chevrel-type phases have been extensively studied because of their outstanding superconducting properties (*1*). Specially interesting are the systems containing rare-earth elements, since they may exhibit superconductivity in spite of the large concentration of rare-earth ions (*2*).

Most of the studies of R–Mo–*X* (R = rare-earth; X = chalcogenide) systems have been performed on compacted powders sintered at 1100–1250°C. However, even though the chemistry and crystal structures appear to be well characterized, discrepancies in the stoichiometry and its associated properties often occur. To understand the complex behavior of these compounds, it is sometimes necessary to use single-crystal samples for measurements of the physical properties. Unfortunately, the high chemical reactivity of these materials, and their tendency to decomposition make the preparation of single crystals very difficult.

Continuing our program on crystal growth (*3*) of rare-earth molybdenum sulfides, we focused on the $EuMo_6S_8$ phase since the case of europium is one of the most unusual and controversial among the R–Mo–X series. At atmospheric pressure, europium and cerium compounds are the only ones which are not superconductors. At $T_s \simeq 110$ K, $EuMo_6S_8$ undergoes a structural transformation from a room-tempera-

[1] To whom correspondence should be addressed.

[2] Permanent address: Institute for Low Temperature and Structure Research of the Polish Academy of Sciences, 1, plac Katedralny, 50-950 Wroclaw, Poland.

0022-4596/86 $3.00

ture rhombohedral structure to a triclinic structure (*4*). The high-temperature phase is metallic in character while, in the triclinic phase, the resistivity increases rapidly at low temperatures. Under pressure, the crystallographic transformation seems to be much inhibited: T_s decreases with pressure, and $EuMo_6S_8$ becomes superconducting at about 10 kbar (*5, 6*). However, doubts arose when superconductivity was associated with impurities present in powdered sintered samples of different and not well-defined stoichiometries (*7*). Later, Decroux *et al.* (*8*) ruled out this last hypothesis when performing high-pressure investigations on melted samples of $EuMo_6S_8$. They ascribed this phenomenon to bulk superconductivity of the Chevrel phase. Very recently, Holtzberg *et al.* (*9*) prepared very small single crystals of $EuMo_6S_8$ which did not show the large increase of resistivity in the triclinic phase, but instead they exhibited a metallic behavior at low temperature.

In this work, we report single-crystal data and refinement of the crystal structure of $EuMo_6S_8$ and, in addition, physical characterization by means of susceptibility and resistivity measurements above 2 K under zero pressure.

Crystal Structure

1. Experimental Details

Molybdenum disulfide, europium sulfide, and molybdenum metal prepared by standard techniques, were mixed in appropriate quantities to obtain the stoichiometric formula $Eu_{1.0}Mo_6S_8$. They were pressed into pellets and reacted at 1200°C in an ordinary resistance furnace. Mechanical mixtures of $EuMo_6S_8$ and EuS were then prepared as starting materials for crystallization. The quantity of europium sulfide in the mixture was of the order of 0.5 to 2 times its percentage in the Chevrel phase.

Crystallization was performed with approximately the same method which had been used in the Ho–Mo–S system (*3*). This time, however, the crystal growth technique was simplified and experiments were carried out under normal pressure of argon. As before, the starting material decomposes at high temperatures and it shifts its overall composition toward the field of primary crystallization of the Chevrel phase (*3*). In order to determine this speed of decomposition, we performed preliminary experiments on the binary component Mo–S (*11*), which revealed that the sulfur evaporation rate is drastically diminished as soon as the Mo_2S_3 composition is reached, and it stays fairly constant within a wide range of concentrations, including Mo–50 at/o S (for instance, at 1600°C, sulfur losses are less than 1 at/o S per hour). Since the sulfur concentration in Chevrel phases lies within this region (53.33 at/o S), similar conclusions could be assumed for the ternary system. Obviously, the decomposition rate can increase when melting, but nevertheless it will be the liquid phase which will loose its sulfur, and not the solid phase crystallizing out of it. Then, in order to keep the liquid phase saturated with the solid phase throughout the process of crystallization, a suitable speed of cooling should be maintained.

Based on these factors, this new technique of crystallization seems to be a quite universal one, as far as the rare earth molybdenum sulfides are concerned. Up to now, we have successfully used it in other systems, such as $HoMo_6S_8$, $CeMo_6S_8$, and $ErMo_6S_8$, besides $EuMo_6S_8$ which is presented on this work. A detailed report of this new method and on phase equilibria relations in some *R*–Mo–S ternary systems is under preparation and will be published elsewhere (*11*).

Using the new approach, we got large irregular polycrystals of $EuMo_6S_8$ of sizes up to 10 mm^3, together with elongated single crystals of a few millimeters in length. Av-

TABLE I

CRYSTAL DATA FOR $EuMo_6S_8$[a]

Space group	$R\bar{3}$	
	$Z = 1$	
Unit cell dimensions	$a_R = 6.5531(2)$ Å	$a_H = 9,1806(9)$ Å
	$\alpha_R = 88.931(5)°$	$c_H = 11.5601(7)$ Å
	$V_R = 281.26(3)$ Å^3	$V_H = 843.77(2)$ Å^3
Crystal dimensions (mm^3)		0.1 × 0.1 × 0.1
$\mu\bar{R}$		0.85
Mo$K\bar{\alpha}$ radiation (λ (Å))		0.71073
Scan method		$\omega - 2\theta$
Reciprocal space		$\theta < 35°$
Independent reflections ($I > \sigma(I)$)		890
Reliability factors R		0.024
R_w		0.047
Goodness of fit		1.329
Europium occupancy at the origin site n		0.998(2)

[a] A list of observed and calculated structure factors can be obtained from the authors.

erage weight of monophased pieces was up to 10 to 20 mg. The crystals were qualitatively microanalyzed using a JEOL JSM-35 CF scanning electron microscope equipped with a TRACOR energy-dispersive-type X-ray spectrometer.

Three single crystals coming from different experiments were selected for structure analysis and refinement with an Enraf-Nonius CAD-4 X-ray diffractometer. The cell parameters of all these crystals were equivalent, and one of them was chosen for structural determination. The data collection parameters for this specimen are given in Table 1. The intensities were corrected for the Lorenz-polarization factor. No absorption correction was applied because of the small size of the crystal ($\mu\bar{R} < 1$).

2. *Solution and Refinement of the Structure*

The structure was solved using an SDP program adapted for a PDP 11/60 minicomputer. The data were analyzed as described in Ref. (*12*). Refinement of the europium occupancy at the origin site showed its complete occupation (n(Eu) = 0.998(2)). A final difference map did not show any residual peak above 1.5 electrons Å^{-3}. The atomic positions and anisotropic temperature factors for the four independent atoms are given in Table II.

The first important result obtained from the crystal structure data concerns the upper limit of existence of the $Eu_xMo_6S_8$ phase. The experimental conditions of crystal growth were such that there was always an excess of the EuS phase in the starting material subjected to melting. Nevertheless, the europium occupancy at the origin site was found equal to unity with no occupation of secondary sites. Thus, we conclude that the europium concentration never exceeds 1.0, regardless of the excess of rare-earth sulfide in the starting material. This result confirms our previous conclusions (*10, 12*) about the maximum concentration of the rare-earth in Chevrel phases. On the other hand, no conclusion can be

TABLE II

POSITIONAL PARAMETERS AND REFINED TEMPERATURE FACTORS[a]

Atom	x	y	z	Beq (Å^2)	$\beta_{11} \times 10^5$	$\beta_{22} \times 10^5$	$\beta_{33} \times 10^5$	$\beta_{12} \times 10^5$	$\beta_{13} \times 10^5$	$\beta_{23} \times 10^5$
Mo	0.22863(4)	0.41817(4)	0.56278(4)	0.478(4)	281(5)	285(5)	271(5)	−33(8)	−68(8)	−63(8)
S(1)	0.3822(1)	0.1251(1)	0.7436(1)	0.64(1)	430(10)	300(10)	400(10)	−11(20)	0(2)	70(20)
S(2)	0.2447(1)	—	—	0.780(5)	460(10)	460(10)	460(10)	−210(20)	−210(20)	−210(20)
Eu	0	—	—	1.142(2)	672(4)	672(4)	672(4)	−411(7)	−411(7)	−411(7)

[a] The data are defined in space group $R\bar{3}$. The estimated standard deviations are given in parentheses. The thermal factor is given by: $\exp\{-(\beta_{11}h^2 + \beta_{22}k^2 + \beta_{33}l^2 + \beta_{12}hk + \beta_{13}hl + \beta_{23}kl)\}$. The equivalent thermal parameter is defined by

$$B\text{eq} = 4/3 \sum_i \sum_j \beta_{ij} a_i a_j.$$

drawn about the lower limit of homogeneity on $Eu_xMo_6S_8$. As stated above, an essential condition needed to obtain large single crystals from the melt is to act against the internal decomposition by using a rare-earth sulfide excess. Therefore, in the present state of the research, we cannot control a substoichiometry, at least in large single crystals. Very small single crystals of $Ho_{0.88}Mo_6S_8$ (*10*) were obtained, however, by partial melting of stoichiometric sintered powder. Thus, a finite domain of existence below $x = 1.0$ may also occur in $Eu_xMo_6S_8$, which would explain some different transport properties observed on sintered powder (*13*), melted samples (*4*), or single crystals (*9*).

An additional hint that physical effects may depend strongly on europium concentration derives from the fact that the lattice parameters published for "stoichiometric" $EuMo_6S_8$ differ enormously from one report to another. For instance, the reported cell volume V_R of the rhombohedral lattice goes from 278.5 to 280 Å^3 in sintered powders (*2*) to 281–283 Å^3 in melted samples (*4, 14*), that is a 1.6% variation of the cell volume due to different preparation techniques.[3] For comparison, the cell volumes of well-characterized $Ho_xMo_6S_8$ single crystals differ by approximately 0.5% for such extreme cases as $x = 0.88$ and $x = 1.0$ (*10*) or $x = 0.67$ and $x = 0.94$ (*15*).

The room temperature crystal structure of $EuMo_6S_8$ can be described in the same way as other Chevrel-type phases with large cations (*16*): two Mo_6S_8 units and a EuS_8 cubic site stacked along the threefold axis of an hexagonal-rhombohedral unit cell, as shown in Fig. 1. Some of the characteristic interatomic distances in $EuMo_6S_8$ are listed in Table III. In Table IV, we compare the main (Mo–Mo) distances of Eu Mo_6S_8 to other divalent and trivalent Me

[3] The three crystals investigated in our different experiments had 281.3 Å$^3 \leqq V_R \leqq$ 282.0 Å^3, suggesting well reproducible europium contents.

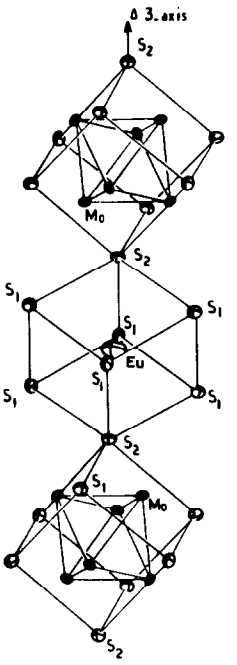

FIG. 1. Crystal structure of $EuMo_6S_8$; two Mo_6S_8 units and one EuS_8 cubic site are shown. The S(2) atoms are situated along the threefold axis.

Mo_6S_8 (Me = metal) as a function of the cell volumes. For this comparison, we have selected well-known divalent and trivalent cations, with no delocalization of the metal atom around the origin site. At a first glance, we can notice that the intracluster Mo–Mo distances are not very crucial in fixing the volume of the unit cell: the size of a molybdenum triangle perpendicular to the ternary axis remains unchanged, while the distance between two such triangles within a Mo_6 octahedron increases slightly for divalent cations (with the exception of the barium compound). This behavior has been noticed in the lanthanides series (*12*) and corresponds to an elongation of the Mo_6S_8 unit when the cation valence decreases (*16*). More critical variation can be noticed on the Mo–Mo intercluster distances: trivalent Gd and Er compounds have rather short distances, when compared to their neighbor lanthanides Eu^{2+} and Yb^{2+}. This

TABLE III

SHORTEST INTERATOMIC DISTANCES (IN Å) IN $EuMo_6S_8$

Mo_6S_8 cube		
	$(Mo-Mo)_\Delta$ intra[a]	2 × 2.665(1)
	$(Mo_\Delta-Mo_\Delta)$ intra[b]	2 × 2.716(1)
	(Mo–Mo) inter[c]	3.278(1)
	(Mo–S(1)) intra	2.448(1)
		2.460(1)
		2.508(1)
	(Mo–S(1)) inter	2.583(1)
	Mo–S(2)	2.391(1)
EuS_8 cube		
	Eu–S(1)	6 × 3.104(1)
	Eu–S(2)	2 × 2.830(1)

[a] $(Mo-Mo)_\Delta$ intra: atoms belonging to the same Mo_6-cluster and situated on the same plane perpendicular to ternary axis.

[b] $(Mo_\Delta-Mo_\Delta)$ intra: atoms belonging to the same Mo_6-cluster but situated on two neighboring planes.

[c] (Mo–Mo) inter: atoms belonging to neighbor clusters.

means that Mo_6S_8 units are situated further apart in the latter compounds and that the main mechanisms in the volume determination are the intercluster distances rather than the intracluster parameters.

Localization of the europium atom at the origin site does not differ much from the ones found in the RMo_6S_8 series (*10, 12*). The RMS displacement of the thermal vibrations around the origin site perpendicular and parallel to the ternary axis are $\langle X_\perp \rangle = 0.136$ Å and $\langle X_\parallel \rangle = 0.071$ Å, respectively.

Physical Properties at Ambient Pressure

1. Electrical Resistivity

Two crystals from different preparations were selected for electrical resistivity measurements between 4.5 and 300 K. Sample 1, initially of cubic shape, was ground into a flat plate of 0.3 mm thickness, 0.5 × 0.5 mm^2 surface; measurements were performed using alternating currents below 10 mA, in a Van der Pauw configuration. Sample 2 was an elongated crystal of dimensions 0.6 × 0.25 × 0.2 mm^3, with the longest axis along the hexagonal *c*-axis of the crystal structure; direct currents below 2 mA were used in a standard four-point probe geometry.

Figure 2 shows the electrical resistivity of both specimens, normalized to their room temperature values ρ_{amb} (600 and 589 $\mu\Omega$ cm for samples 1 and 2, respectively). A large and well-defined anomaly less than 0.5 K wide is seen at $T_s = 107$ K, due to the structural transition from the rhombohedral to the triclinic structure. The resistivity variation of the high-temperature phase is metal-like, with a broad minimum at 220 K: the resistivity decreases by 1.5% with respect to its room temperature value, and then increases by almost 30% prior to the transition. At the transition, the resistivity of both samples jumps by a factor of 2.

The resistivity behavior of the low-temperature phase differs from one sample to

TABLE IV

MAIN INTERATOMIC DISTANCES (Å)[a] IN SOME DIVALENT AND TRIVALENT $Me^{n+}Mo_6S_8$

	$Ba^{2+}Mo_6S_8$	$Sn^{2+}Mo_6S_8$	$Eu^{2+}Mo_6S_8$	$Gd^{3+}Mo_6S_8$	$Er^{3+}Mo_6S_8$	$Yb^{2+}Mo_6S_8$
V_H (Å^3)	881	834	844	809	803	826
$(Mo-Mo)_\Delta$ intra	2.67	2.688	2.665	2.660	2.660	2.669
$(Mo_\Delta-Mo_\Delta)$ intra	2.70	2.737	2.716	2.714	2.708	2.728
(Mo–Mo) inter	3.41	3.232	3.278	3.163	3.142	3.208
References	*14*	*25*	This work	*26*	*27*	*12*

[a] As defined in Table III.

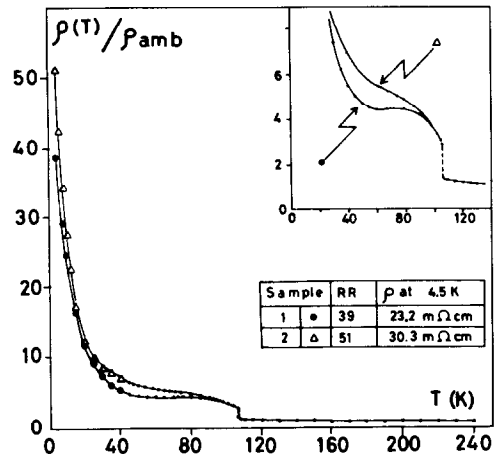

FIG. 2. Normalized resistivity of two stoichiometric $Eu_{1.0}Mo_6S_8$ single crystals. *RR* is defined as $\rho(4.5\text{ K})/\rho(300\text{ K})$. The inset shows the structural transition in detail.

the other, in the range 50 K $< T < T_s$: specimen 1 presents a clear maximum at 75 K followed by a minimum of resistivity at 60 K; sample 2, on the other hand, shows a smooth but definite "shoulder" with an inflection point at approximately 60 K. At lower temperatures, both samples present essentially the same features; that is, a rapid increase of resistivity toward a semiconductor behavior and large resistivity values at 4.5 K (23 and 30 mΩ cm for samples 1 and 2, respectively). It should be noted also that specimen 1 presents a large anisotropy (factor of 2) between 15 and 60 K, when measuring the voltage drop across the sample in two of the Van der Pauw configurations (*17*). For the rest of the temperature range, this anisotropy is less important.

The resistivity behavior of our single crystals is reminiscent of reported results on melted $EuMo_6S_8$ (*4*), in particular the sharp anomaly at T_s (very smooth in sintered powders) and the resistivity minimum at 60 K. Room-temperature resistivity values are similar to those obtained in sintered powders or melted material. The most striking results are, however, our large resistivity ratios $RR \equiv \rho(LT)/\rho_{amb} = 39$ and 51, when measured at $LT = 4.5$ K (for comparison, Meul *et al.* (*18*) obtained $RR = 23.8$ on molten $Eu_{1.1}Mo_6S_8$ at still lower temperatures, $LT = 2$ K).

On the other hand, recent results of Holtzberg *et al.* (*9*) on single crystals of $EuMo_6S_8$ and $EuMo_5WS_8$ show that these phases are essentially metallic at low temperatures, and that, in some crystals, the electrical resistivity decreases as T^2 due to molybdenum spin fluctuations. Such different and opposite behaviors observed in well-crystallized materials should then be ascribed to off-stoichiometry effects, as discussed above. In fact, Harrison *et al.* (*6*) have reported different temperature dependences of the resistance of powdered $Eu_xMo_6S_8$ ($x = 1.0$ and 1.2). According to (*6*), the europium-richest sample shows the nonmetallic behavior usually observed on sintered powders, while the sample containing less europium presents a resistance-versus-temperature curve much alike to the one of Holtzberg, that is, a maximum toward 70 K, followed by a decrease of the resistance at lower temperatures. In the light of the results discussed above concerning the homogeneity domain, the europium concentrations given by (*6*) should be stepped down. It is then quite plausible that such a metal-like behavior would be characteristic of substoichiometric samples. This phenomenon is not new in the physics of rare-earth compounds: semiconducting SmB_6 changes its properties drastically when vacancies are present in the lattice (*19*) and its residual resistivity may change three or four orders of magnitude with sample preparation (*20*); intermediate-valent Tm_xSe ($x \leqq 1.0$) goes from a metallic to an insulator state at $T = 0$ when x approaches 1.0 (*21*); magnetic semiconductor EuO can exhibit a wide range of resistivity behaviors depending on doping and upon deviations from stoichiometry (*22*), just to cite a few examples among others.

In the case of $EuMo_6S_8$, the sample preparation techniques used by the different groups working on crystal growth (*3, 4, 15*) are quite dissimilar, so it becomes difficult to state the main reasons of such difference in europium concentrations. We believe however that due to our method of crystal growth, our materials might have the highest content of europium possible, and that the $Eu_{1.0}Mo_6S_8$ low-temperature phase must be essentially semiconducting.

2. *Susceptibility and Magnetization Measurements*

The magnetic susceptibility of $Eu_{1.0}Mo_6S_8$ crystals was measured down to 4.5 K in a commercial SQUID magnetometer (*23*). The inverse of the susceptibility (Fig. 3) follows a Curie law below 100 K, with an effective moment of 7.95 μ_B/at. Eu, in excellent agreement within experimental error with the theoretical moment of divalent europium (7.94 μ_B). At higher temperatures, the inverse susceptibility deviates slightly from a Curie law, as if a constant susceptibility was superimposed to it. Surprisingly, the bending of the magnetic susceptibility becomes noticeable just above T_s, but the effect is too small to pinpoint any anomaly on the χ^{-1}-versus-T curve. At lower temperatures, a small anomaly (not seen in the figure) centered at 15 K was detected in rough samples taken directly from the melt. This anomaly, likely due to some inclusions of EuS which orders magnetically at 16.5 K, was substantially diminished by plunging the crystals into an HCl : alcohol solution and dissolving the binary sulfide sticking to the surface.

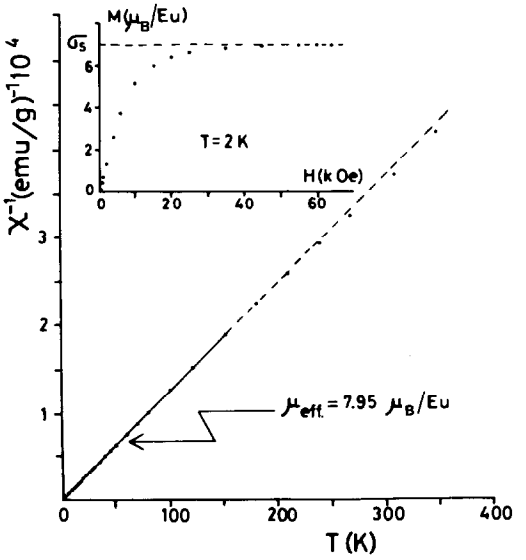

FIG. 3. Inverse magnetic susceptibility of $Eu_{1.0}Mo_6S_8$. The straight line corresponds to a Curie law below 120 K. The inset shows the saturation of the magnetization at 2 K.

Further confirmation of the divalency of all europium atoms comes from magnetization measurements performed as a function of magnetic field at 2 K (insert, Fig. 3). Divalent europium has $S = \frac{7}{2}$, $L = 0$, $J = \frac{7}{2}$ and $g = 2$; the saturation moment of the free ion is 7 μ_B. The $Eu_{1.0}Mo_6S_8$ sample, composed of four single crystals weighing 11.5 mg in total, saturates at the limiting magnetic field (64 kOe) of our susceptometer, with a saturation moment of 7.00 μ_B, in excellent agreement with the expected value.

Conclusion

Reproducible experiments of crystal growth of the $EuMo_6S_8$ phase were performed. First, the crystal structure at room temperature was refined using single-crystal data. Later, a physical characterization of their basic properties, e.g., electrical resistivity and magnetic susceptibility, was done, and compared to those already existing in the literature for sintered powders and melted materials.

The structure analysis reveals that the europium concentration never exceeds the stoichiometric composition $Eu_{1.0}Mo_6S_8$, regardless of the rare-earth concentration of the starting material. The europium atom occupies the origin site of the hexagonal–rhombohedral unit-cell, with no visible de-

localization. All europium atoms are divalent as suggested from the lattice volume, and subsequently confirmed by susceptibility and magnetization measurements. The magnetic susceptibility follows a Curie law below 100 K, and it is superimposed to a constant paramagnetic susceptibility at high temperatures.

The electrical resistivity was measured in two samples from different preparations. While their behaviors are quite similar in the high-temperature metallic phase, they differ markedly at low temperature though keeping the same semiconducting-like features. Resistivity ratios are the largest found in the literature up to now. Other experiments using these single crystals are being performed (*24*) and they confirm—among other properties—a superconducting state under pressure.

Acknowledgments

One of us (R.H.) would like to thank the hospitality shown to him during his stay at Rennes. We are grateful to Dr. M. Potel for his help in refining the crystal structure and to Dr. J. Rossat-Mignod and Dr. R. Tournier for useful and encouraging discussions. This research was supported by the French Direction des Recherches et Etudes Techniques under Contract 84/109.

References

1. "Superconductivity in Ternary Compounds" (Ø. Fischer and M. B. Maple, Eds.), Vols. I and II, Springer, Berlin (1982).
2. Ø. Fischer, A. Treyvaud, R. Chevrel, and M. Sergent, *Solid State Commun.* **17,** 721 (1975).
3. R. Horyn, O. Peña, and M. Sergent, *J. Less-Common Met.* **105,** 55 (1985).
4. R. Baillif, A. Junod, B. Lachal, J. Muller, and K. Yvon, *Solid State Commun.* **40,** 603 (1981).
5. C. W. Chu, S. Z. Huang, C. H. Lin, R. L. Meng, M. K. Wu, and P. H. Schmidt, *Phys. Rev. Lett.* **46,** 276 (1981).
6. D. W. Harrison, K. C. Lim, J. D. Thompson, C. Y. Huang, P. D. Hambourger, and H. L. Luo, *Phys. Rev. Lett.* **46,** 280 (1981).
7. R. W. Mc Callum, W. A. Kalsbach, T. S. Radhakrishnan, F. Pobell, R. N. Shelton, and P. Klavins, *Solid State Commun.* **42,** 819 (1982).
8. M. Decroux, S. E. Lambert, M. S. Torikachvili, M. B. Maple, R. P. Guertin, L. D. Woolf, and R. Baillif, *Phys. Rev. Lett.* **52,** 1563 (1984).
9. F. Holtzberg, J. Flouquet, M. Konczykowski, A. Sulpice, and R. Tournier, *J. Appl. Phys.* **57,** 3067 (1985).
10. O. Peña, R. Horyn, M. Potel, J. Padiou, and M. Sergent, *J. Less-Common Met.* **105,** 105 (1985).
11. R. Horyn, C. Geantet, O. Peña, and M. Sergent, to be published.
12. O. Peña, P. Gougeon, M. Sergent, and R. Horyn, *J. Less-Common Met.* **99,** 225 (1984).
13. M. B. Maple, L. E. Delong, W. A. Fertig, D. C. Johnston, R. W. Mc Callum, and R. N. Shelton, *in* "Valence Instabilities and Related Narrow Band Phenomena" (R. D. Parks, Ed.), pp. 17–29, Plenum, New York (1977).
14. R. Baillif, A. Dunand, J. Muller, and K. Yvon, *Phys. Rev. Lett.* **47,** 672 (1981).
15. F. Holtzberg, S. J. La Placa, T. R. Mc Guire, and R. A. Webb, *J. Appl. Phys.* **55,** 2013 (1984).
16. R. Chevrel and M. Sergent, *Top. Curr. Phys.* **32,** 25 (1982).
17. L. J. Van der Pauw, *Philips Res. Rep.* **13,** 1 (1958).
18. H. W. Meul, M. Decroux, R. Odermatt, R. Noer, and Ø. Fischer, *Phys. Rev. B: Condens. Matter* **26,** 6431 (1982).
19. T. Kasuya, K. Kojima, and M. Kasaya, *in* "Valence Instabilities and Related Narrow Band Phenomena" (R. D. Parks, Ed.), pp. 137–149, Plenum, New York (1977).
20. T. Tanaka, R. Nishitani, C. Oshima, E. Bannai, and S. Kawai, *J. Appl. Phys.* **51,** 3877 (1980).
21. P. Haen, F. Lapierre, J. M. Mignot, R. Tournier, and F. Holtzberg, *Phys. Rev. Lett.* **43,** 304 (1979).
22. M. R. Oliver, J. O. Dimmock, A. L. Mc Whorter, and T. B. Reed, *Phys. Rev. B: Condens. Matter* **5,** 1078 (1972).
23. S.H.E. GmbH, Cryogenic Instruments and Systems, Aachen, FRG, Variable Temperature Susceptometer.
24. J. Beille, personal communication, 1985.
25. R. Chevrel, C. Rossel, and M. Sergent, *J. Less-Common Met.* **72,** 31 (1980).
26. K. Yvon, *Curr. Top. Mater. Sci.* **3,** 55 (1979).
27. C. Geantet, O. Peña, M. Sergent, and R. Horyn, to be published.